

---

**HIGH MULTIPLICITY INFLUENCE ON THE PION-PION  
FINAL STATE INTERACTIONS IN RELATIVISTIC  
HEAVY ION COLLISIONS**

**D. V. ANCHISHKIN, W. A. ZAJC<sup>1</sup>, G. M. ZINOVJEV**

UDC 538.9; 538.915; 517.957  
© 2002

**Bogolyubov Institute for Theoretical Physics, Nat. Acad. Sci. of Ukraine**  
(14b, Metrolohichna Str., 03143 Kyiv, Ukraine),

<sup>1</sup>**Nevis Laboratories, Columbia University**  
(Irvington, NY 10533, USA)

---

The corrections for two pion correlations due to electromagnetic final state interactions are investigated for high secondary multiplicities relevant for relativistic heavy ion collisions. The analysis is based on the numerical solutions of the Schrödinger equation exploiting a two-particle potential which is distorted by the multiparticle environment. Two different post freeze-out scenarios are examined. First, it is shown that the presence of a uniform and static post freeze-out medium results in a noticeable deviation from the standard Gamov factor (this factor, which is independent from a particular model, is taken as an indicator of two-particle electromagnetic final state interactions). Second, after the passage to a more realistic model which mimics the expansion of the multipion system, we come to the opposite conclusion. Because the density of the secondary particles drops down faster than  $1/R^2$ , where  $R$  is the distance from the fireball, the pion pair promptly escapes the initial high density region and the distortion of mutual Coulomb potential is weak. It is shown that even overestimating the density of the post freeze-out environment the correction factors obtained for SPS and LHC freeze-out conditions differ from the standard Gamov factor just in several percent.

---

**Introduction**

Two-particle correlations provide information about the space-time structure and dynamics of the emitting source [1]. For a further consideration of correlations which occur in relativistic heavy ion collisions (RHIC), let us assume that the particles are emitted independently (or the source is completely chaotic). Then, the correlations reflect a) the effects from symmetrization (antisymmetrization) of the amplitude to detect identical particles with certain momenta, and b) the effects which are generated by the final

state interactions of the detected particles between themselves and with the source. On the first sight, one can regard the final state interactions (FSI) as a contamination of “pure” particle correlations. But, it should be pointed that the FSI depend on the structure of the emitting source and thus provide information about the source dynamics as well. In fact, this was proved by intensive investigation during last twenty years of two-particle and source-particle FSI [1, 2] (for recent publications see, for example: a) Two-particle FSI: [3] and references therein; b) Source-particle FSI: [4, 5] and references therein).

Actually, the former approaches accounting for FSI deal with secondaries in the empty post freeze-out space. Meanwhile, even in modern SPS experiments, for instance Pb + Pb at 160 GeV×A, there were created 800-900 secondary pions which form the obviously plasma-like post freeze-out medium. That is why, it is expected that the FSI, for example, of two separated pions, at this energy and, of course, at the energies of coming RHIC and LHC would be much influenced by the environment formed by other particles. The goal of the present paper is to estimate how strong could be the consequences of the presence of the large number of secondary charged particles on the Coulomb final state interactions. To be independent as much as possible from the source models, we choose the Gamov factor as a standard quantity for estimation which takes into account the Coulomb FSI.

The fundamental observable for intensity interferometry in hadron physics is the relative momentum spectrum of identical particles. For two like-sign pions, the final-state Coulomb interaction modifications to this spectrum result in a correction which has typically been considered as tractable and relatively accurate. This assumption was based on the significantly different length scales between strong ( $\propto 1/m_\pi$ ) and Coulomb ( $\propto 1/m_\pi\alpha$ ) interactions [6, 7] (here  $m_\pi$  is the pion mass and  $\alpha$  represents the fine structure constant). The correction may then be treated on the base of the Schrödinger equation, resulting in the well-known Gamov factor  $G(\mathbf{q})$ :

$$G(|\mathbf{q}|) = |\psi_{\mathbf{q}}(\mathbf{r} = 0)|^2 = \frac{2\pi\eta}{e^{2\pi\eta} - 1}, \quad (1)$$

where  $\psi_{\mathbf{q}}(\mathbf{r})$  is the wave function,  $\eta = \alpha m_\pi/|\mathbf{q}|$ , with  $\mathbf{q}$  as the relative momentum of the particles.

The nominal quantity expressing the correlation function in terms of experimental distributions [1],

$$C(\mathbf{k}_1, \mathbf{k}_2) = \frac{P_2(\mathbf{k}_1, \mathbf{k}_2)}{P_1(\mathbf{k}_1) P_1(\mathbf{k}_2)}, \quad (2)$$

where  $P_1(\mathbf{k}) = E d^3N/d^3k$  and  $P_2(\mathbf{k}_1, \mathbf{k}_2) = E_1 E_2 d^6N/d^3k_1 d^3k_2$  are single- and two-pion cross-sections, is then given (due to the factorization of the corresponding matrix element) in terms of the product of the Gamov factor multiplying the model correlations [2, 3] as

$$C(\mathbf{k}_1, \mathbf{k}_2) = G(|\mathbf{k}_1 - \mathbf{k}_2|) C_{\text{model}}(\mathbf{k}_1, \mathbf{k}_2). \quad (3)$$

It should be mentioned that, in terms of the pion momentum  $\mathbf{k} = \mathbf{k}_1 = -\mathbf{k}_2$ , the modulus of the relative pion momentum  $\mathbf{q} = 2\mathbf{k}$  in the pair center-of-mass system coincides with the invariant relative momentum  $q_{\text{inv}} \equiv [(k_1 + k_2)^2 - 4m_\pi^2]^{1/2}$ , where  $k_1$  and  $k_2$  are the pion four-momenta in an arbitrary frame.

In order to prevent a confusion of different physical reasons on the results obtained, we consider corrections due to the Coulomb final state interactions within a traditional scheme, that is, we do not take into account the finite size of the fireball (for consistent treatment of the source finite size effects, see, for example, [3]). On the evaluation level, it means that we calculate the correction factor in accordance with the formula  $G_{\text{corr}}(|\mathbf{q}|) = |\psi_{\mathbf{q}}(\mathbf{r} = 0)|^2$ , where  $\psi_{\mathbf{q}}(\mathbf{r})$  is obtained from a numerical solution of the Schrödinger equation with the two-particle Coulomb potential which is distorted by the multipion environment. Moreover, as shown in Refs. [9, 10], pions with small relative momentum are

dominantly emitted from the region of homogeneity, i.e., within a space area 1 – 3 fm in length. Hence, for such a pion pair, the “point-like” approximation of the source looks good enough because the wave function is almost constant  $\psi(r = 0) \approx \psi(r = 3 \text{ fm})$  at a relevant spatial interval.

## 1. Uniform Multiparticle Environment

First scenario suggests the uniform post freeze-out multiparticle medium - all space is filled by the hot pion gas of the uniform and static density which is equal to freeze-out one at freeze-out temperature  $T_f$ . Then, the relation between the two-particle electromagnetic potential  $\phi(r)$  and the local charge density is given by

$$\nabla^2 \phi(\mathbf{r}) = -4\pi e \left( n^{(+)} - n^{(-)} \right), \quad (4)$$

where  $e = \sqrt{\alpha}$  is the elementary charge, the density of charged pions  $n^{(\pm)}$  is related to that of neutral pions  $n^{(0)}$  via the Boltzmann factor:

$$n^{(\pm)} = n^{(0)} \exp\left(\mp \frac{e\phi}{T_f}\right). \quad (5)$$

The density  $n^{(0)}$  of  $\pi^0$ -mesons at the freeze-out temperature  $T_f$  coincides with the equilibrium density of charged pions in absence of Coulomb interactions (we consider symmetric nuclear matter). In the limit  $e\phi \ll T_f$ , Eq.(5) can be rewritten as

$$n^{(\pm)} = n^{(0)} \left( 1 \mp \frac{e\phi}{T_f} \right), \quad (6)$$

(this requires that the pions are not closer than  $\sim 10^{-2}$  fm to one another at  $T_f \approx 200$  MeV) so that

$$\nabla^2 \phi(\mathbf{r}) = \frac{8\pi e^2 n^{(0)}}{T_f} \phi(\mathbf{r}). \quad (7)$$

It's solution is well known and given by a screened Coulomb potential

$$\phi_{\pi^\pm}(r) = \pm e \frac{e^{-r/R_{scr}}}{r}, \quad (8)$$

where

$$\frac{1}{R_{scr}} = \sqrt{\frac{8\pi}{3}} \alpha \cdot \sqrt{\frac{n_\pi}{T_f}} \quad (9)$$

with  $n_\pi$  as the total pion density ( $n^{(0)} = n_\pi/3$ ). Thus, for like-sign pions, the potential energy reads

$$U_{\pi\pi}(r) = \frac{\alpha}{r} \exp\left(-\frac{r}{R_{scr}}\right). \quad (10)$$

To evaluate the correction (Gamov) factor, we will subsequently use the screened Coulomb potential (10) to numerically resolve the Schrödinger equation. In turn, this requires an estimate of the pion density and freeze-out temperature. We evaluate this for the extreme case and idealized scenario [12], i.e., just after freeze-out, when pions occupy the volume ( $T_f = 190$  MeV)

$$V_f = \pi R_f^2 2\tau_f \sinh \frac{\Delta y}{2}, \quad (11)$$

and  $R_f = R_{Pb} \approx 7.1$  fm,  $\tau_f = 10$  fm and  $\Delta y \approx 6$  for Pb-Pb collisions. For multiplicities, we assume [13]: 1) LHC:  $N_\pi = 8000$ , 2) SPS:  $N_\pi = 800 \div 1000$ , resulting in screening radii respectively - LHC:  $R_{scr} \approx 7.9$  fm, SPS:  $R_{scr} \approx 25$  fm. The latter may look a bit controversial at first sight (though  $R_{scr} = \infty$  for a pure Coulomb interaction). Indeed, using Eq. (11) for the unit interval of rapidity (one might consider that more natural, in a sense), we obtain a much smaller value of the corresponding screening radius. None the less, we cite this quantity here as an upper bound under existing experimental conditions.

The results of these calculations are plotted in Fig. 1 together with the standard Gamov factor. We also show a curve obtained by use of NA44 experimental values [14]:  $T_f = 187$  MeV,  $\tau_f = R_L \approx 6.0$  fm,  $R_T = 6.0$  fm,  $\Delta y = 3$  and  $dN/dy = 40$ . These parameters produce an even smaller screening radius ( $R_{scr} \approx 19.3$  fm) than our nominal SPS value, and hence a larger correction to the standard Gamov factor. Based on these considerations, it appears that a substantial correction to the standard Gamov factor is already required by the existing experimental data. This is particularly true for kaon interferometry since the pion medium also screens the K-K Coulomb final state interaction, and the length scale of the K-K Gamov factor is larger than that for pions by their mass ratio. In fact, it is seen a not so big difference from the evaluation of  $G_{corr}(Q)$  for the same screened potential with making use of the quasiclassical approximation [15].

Actually, what we really obtained from our consideration of this idealized foregoing scenario (constant and uniform spatial density of the environment) is that the cancelation of the Coulomb potential tail (by screening) results in an increase of the correction factor in the region of small relative momenta ( $Q \leq 50$  MeV) as seen from Fig. 1. So, the long distance behavior of the potential is responsible for the dramatic deviation of the correction factor for small relative momenta from standard Gamov, which is calculated in the absence of screening environment

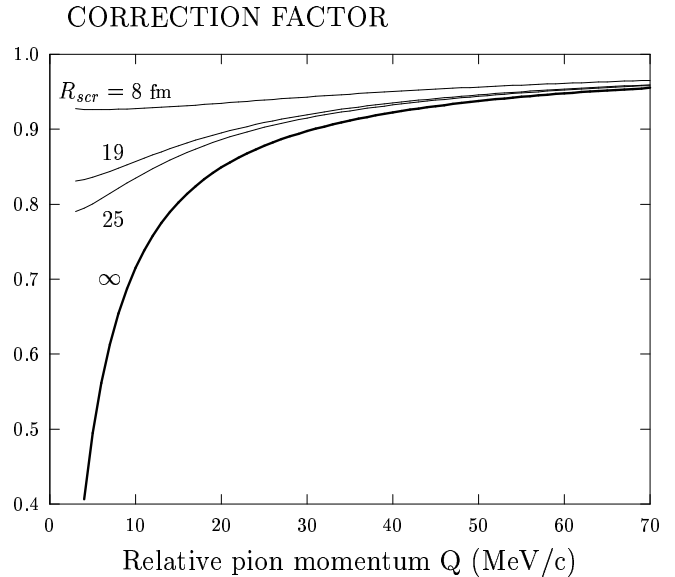


Fig. 1. Correction factor  $G_{cor}(Q)$  versus relative pion momentum. Correction factor  $G_{cor}(Q) = |\psi(\mathbf{r} = 0)|^2$  was obtained by solving the Schrödinger equation with the use of screened Coulomb potential (10). Curves depicted are evaluated for the different freeze-out conditions: 1) LHC conditions:  $N_\pi = 8000$ ,  $T_f = 190$  MeV and  $R_f = 7.1$  fm, what gives  $R_{scr} = 7.9$  fm, 2) Experimental values obtained by NA44 [14]:  $T_f = 187$  MeV,  $\tau_f = R_L \approx 6.0$  fm,  $R_T = 6.0$  fm,  $\Delta y = 3$  and  $dN/dy = 40$ , what gives  $R_{scr} = 19.3$  fm, 3) SPS conditions:  $N_\pi = 800$ ,  $T_f = 190$  MeV and  $R_f = 7.0$  fm, what gives  $R_{scr} = 25$  fm. Bottom curve is the standard Gamov factor ( $R_{scr} = \infty$ )

( $R_{scr} = \infty$ ). Meanwhile, the tail of the two-particle potential gives the main contribution into the interaction when two particles are far from one another and thus they are far from the fireball. On the other hand, in the realistic scenario the density of secondary particles or the density of environment drops down faster than  $1/R^2$ , where  $R$  is the distance from the fireball. Hence, the distortion of mutual Coulomb potential for two charged pions decreases with increase of  $R$  and consequently with increase of the distance between particles. So, we can conclude that in reality a distortion (screening) of the tail of the Coulomb potential is much weaker than in the model with uniform medium density considered above and thus it is supposed that the distortion of the Gamov factor is not so dramatic. To keep this qualitative speculation as a thread, we next turn to a more realistic model which mimics the expansion after freeze-out.

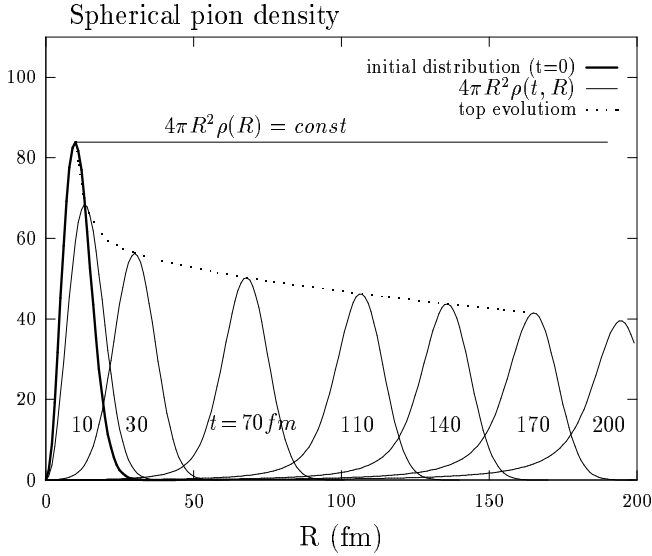


Fig. 2. Dependence of the spherical pion density  $\rho_{\text{sph}}(t, R) \equiv 4\pi R^2 \rho(t, R)$  on  $R$ , where  $\rho(t, R)$  is the number of pions in the unit volume at the time  $t$  and at the distance  $R$  from the center of the fireball ( $\int_0^\infty dR \rho_{\text{sph}}(t, R) = N_\pi$ ). The density was evaluated for initial data (SPS conditions):  $N_\pi = 1000$ ,  $T_f = 190$  MeV and  $R_f = 7$  fm. The spherical pion density is depicted for the times (solid Gaussian-like curves): 1) initial distribution,  $t = 0$ , 2)  $t = 10$  fm, 3)  $t = 30$  fm, 4)  $t = 70$  fm, 5)  $t = 110$  fm, 6)  $t = 140$  fm, 7)  $t = 170$  fm, 8)  $t = 200$  fm. Dotted curve is the evolution of the tops of spatial pion distributions. Straight solid line in the top, which is parallel to x-axis, is some constant spherical density  $\rho_{\text{sph}}(t, R) = 4\pi R^2 \rho(R) = \text{const}$

## 2. Expansion Scenario

In the previous scenario, all position space was filled up by particles with the constant density. This is, certainly, a very rough approximation. To take into account the spherical expansion of the pion system, we parametrize the pion density after freeze-out as

$$n(R) = n_f \frac{R_f^2}{R^2}, \quad (12)$$

where  $n_f$  is the freeze-out pion density,  $R_f$  and  $T_f$  are the freeze-out radius and temperature.

To establish this dependence of the density on the distance from the fireball, let us consider the classical phase-space distribution function of pions. After freeze-out, it satisfies the collisionless Boltzmann kinetic equation

$$\frac{\partial f(x, p)}{\partial x_0} + \mathbf{v} \cdot \nabla f(x, p) = 0, \quad (13)$$

where  $\mathbf{v} = \mathbf{p}/E$  is the velocity of a particle and  $E = \sqrt{m^2 + \mathbf{p}^2}$  is its energy. We look for the expansion solution of this equation which can be fixed by an asymptotic condition, for instance,  $\lim_{t \rightarrow \infty} f(t, \mathbf{x} = 0; \mathbf{p}) = 0$ . A solution of this type can be written in the form

$$f(t, \mathbf{R}, \mathbf{p}) = f_0(\mathbf{R} - \mathbf{v}t, \mathbf{p}), \quad (14)$$

where  $f_0(\mathbf{R}, \mathbf{p})$  is the initial distribution ( $t = 0$ ). We take the initial distribution as simple as possible: Let us assume that the particles were distributed just before freeze-out (a) in accordance with the Boltzmann law in the momentum space, and (b) in accordance with the Gaussian law in the position space. The taken accuracy (classical kinetic equation) is quite enough to describe the *collective* (!) behavior of the pion system after freeze-out. So, we adopt that, at time  $t = 0$ , the system shall occupy phase space according to the distinct distribution function

$$f_0(\mathbf{R}, \mathbf{p}) = \rho_0(\mathbf{R})g_0(\mathbf{p}), \quad (15)$$

where

$$\rho_0(\mathbf{R}) = \frac{N_\pi}{(2\pi R_f^2)^{3/2}} \exp\left(-\frac{R^2}{2R_f^2}\right), \quad (16)$$

with  $\int d^3R \rho_0(\mathbf{R}) = N_\pi$ , and

$$g_0(\mathbf{p}) = \frac{2\pi^2}{m^2 T_f K_2\left(\frac{m}{T_f}\right)} \exp\left(-\frac{\sqrt{m^2 + \mathbf{p}^2}}{T_f}\right), \quad (17)$$

with  $\int [d^3p/(2\pi)^3] g_0(\mathbf{p}) = 1$  and  $R = |\mathbf{R}|$ . Here,  $N_\pi$  is the number of the pions in the system,  $T_f$  and  $R_f$  are temperature and mean size of the system at the time  $t = 0$  (freeze-out), respectively,  $m$  is the pion mass and  $K_2$  is the McDonald function of the second order.

The space distribution of the particles at any time  $t$  is determined by the integral over the momentum space

$$\rho(t, \mathbf{R}) = \int \frac{d^3p}{(2\pi)^3} \rho_0(\mathbf{R} - \mathbf{v}t)g_0(\mathbf{p}). \quad (18)$$

Due to the spherical symmetry, it is reasonable to look at the radial density of pions

$$\rho_{\text{sph}}(t, R) \equiv 4\pi R^2 \rho(t, R). \quad (19)$$

This quantity may be treated as the number of pions in a shell with unit width at the time  $t$  and the distance  $R = |\mathbf{R}|$  from the fireball center. Hence, it is the one-dimensional spatial distribution function and, evidently, the area under this curve at any time is equal

to the particle number  $N_\pi$  because of normalization  $\int_0^\infty dR \rho_{\text{sph}}(t, R) = N_\pi$ . We evaluate this function in accordance with Eq. (18) just for *SPS* conditions:  $N_\pi = 1000$ ,  $T_f = 190$  MeV and  $R_f = 7$  fm. The result of calculations for different times shown in Fig. 2. It is seen that the distribution looks like Gaussian, whose maximum moves with a velocity very close to the velocity of light. Straight line, which is parallel to the x-axis is some constant spherical density  $4\pi R^2 \rho(R) = \text{const}$ . One can put the 3-dimensional spatial density  $\rho(R)$  in correspondence to this spherical density and get

$$\rho(R) = \frac{\text{const}}{4\pi R^2}, \quad (20)$$

where for the SPS initial conditions depicted in Fig. 2,  $\text{const} \approx 85 \text{ fm}^{-1}$ . Evidently, the spherical density  $\rho_{\text{sph}}(R) = \text{const}$  (horizontal line) at any fixed time is higher than the real particle density of the expanding many-particle system, which in Fig. 2 looks like the Gaussian curves (Gaussian shells). Hence, the spatial density  $\rho(R)$ , which corresponds to the spherical density  $\rho_{\text{sph}}(R) = \text{const}$  in accordance with (20), is higher than the spatial density of the expanding many-particle system. After this, we can state that the adopted law (12) (density profile) of the dependence of the spatial pion density on the distance from the fireball center is *the essential overestimation* of the real pion density at any times.

Let us discuss the meaning of a spherical density which is constant. The horizontal line in Fig. 2 which corresponds to the constant spherical density,  $\rho_{\text{sph}}(R) = \text{const}$ , will reflect the many-particle system without any dispersion of the radial particle velocity. Indeed, if particles of the system move only along the radial directions with radial velocities of the same modulus  $v$  then, the distance between two particles which move along the same radius is constant. We can write the number of particles  $dN$  which belong to the solid angle  $\Omega$  (particle trajectories do not leave this solid angle) and shell of the thickness  $dR$ :  $dN = \rho(R) dV = \rho(R) \Omega R^2 dR$ . The particles which confined to this volume will not cross the borders of the volume during expansion. Thus, if we take after some time the separated group of particles, which characterizes now by the radius  $R'$ , we can write:  $\rho(R) \Omega R^2 dR = \rho(R') \Omega R'^2 dR'$ , because  $dN = dN'$  and  $dR = dR'$ . This results in the following dependence of the spatial particle density on the radius  $R$  (density profile):

$$\rho(R) = \frac{\rho(R') R'^2}{R^2}. \quad (21)$$

As we see from (21), the spherical particle density  $\rho_{\text{sph}}(R)$  of this specific system is obviously constant, and we would obtain for this case that the time evolution of the initial spatial distribution (see Fig. 2) will result in a shift to the right without distortion of the initial density profile shape. Meanwhile, the dispersity of the initial distribution in momentum space results for the real system in a smearing with time of the initial spatial distribution, as we see it in Fig. 2 (in contrast to the above example of the idealized system where all particles have unique radial velocity  $v$ ).

So, to mimic the features of the expansion of many-particle system we shall consider the following model: all space is filled by the pion gas with stationary spatial density profile (12), where the parameter  $n_f$  is the freeze-out particle density which in turn is the initial spatial particle distribution for expansion of the system in free space. Our further goal is to show that even this essential overestimation of the real pion density (see Fig. 2) will not give a noticeable distortion to the electromagnetic two-particle final state interaction, which we will indicate by distortion of the Gamov factor.

If one adopts this picture, then the corresponding scalar electromagnetic potential is a solution of the Maxwell equation (7) with the pion density  $n_\pi$  which depends on  $R$

$$\nabla^2 \phi(\mathbf{r}) = \frac{8\pi\alpha}{3T_f} n(R) \phi(\mathbf{r}), \quad (22)$$

where  $n(R)$  is a total density of pions determined in (12) with  $n_f = n_\pi$ . Introducing the distance  $r$  between two detected particles, we have

$$R \approx R_f + v_{\text{c.m.}} \cdot t, \quad r \approx v_{\text{rel}} \cdot t, \quad (23)$$

where  $v_{\text{c.m.}}$  is the velocity of the two-particle center-of-mass in the fireball rest frame and  $v_{\text{rel}}$  is the relative velocity of the particles ( $v_{\text{rel}} = Q/m$ ,  $t = 0$  is fixed on the freeze-out hyper-surface;  $Q$  is the relative momentum). By exclusion the time  $t$  from the formula (23) we come to the relation

$$R = R_f + \frac{v_{\text{c.m.}}}{v_{\text{rel}}} \cdot r, \quad (24)$$

which means that we parametrize the time evolution by the distance between two separated particles,  $r$ . Thus, one can rewrite the dependence of the pion density on  $R$  as

$$n(R) = \left( \frac{v_{\text{rel}}}{v_{\text{c.m.}}} \right)^2 \frac{n_\pi R_f^2}{(r + \bar{r})^2}, \quad (25)$$

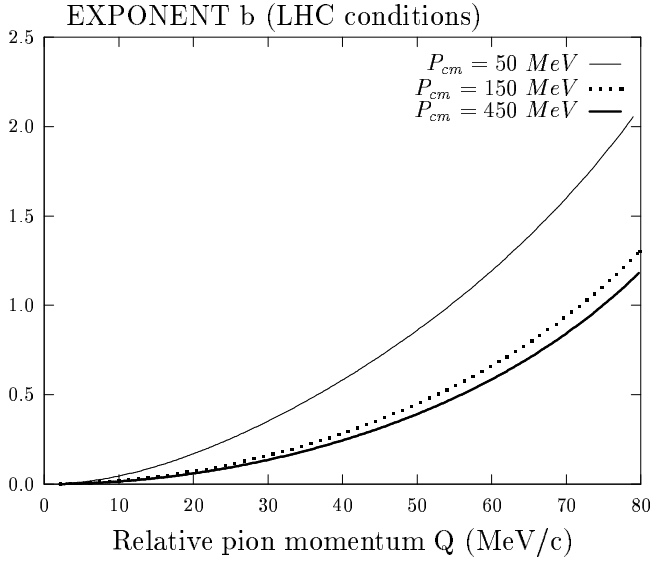


Fig. 3. Exponent  $b$  versus relative pion momentum  $Q$  (see, (32)) for the LHC freeze-out conditions:  $N_\pi = 8000$ ,  $T_f = 190$  MeV and  $R_f = 7$  fm. Every curve was evaluated for particular value of the mean momentum  $P_{c.m.}$  of the pion pair:  $P_{c.m.} = 50$  MeV/c (top),  $P_{c.m.} = 150$  MeV/c (middle),  $P_{c.m.} = 450$  MeV/c (bottom)

where  $\bar{r} \equiv (v_{rel}/v_{c.m.})R_f$  by definition. So, Eq.(22) may be rewritten as

$$\nabla^2 \phi(\mathbf{r}) = \frac{c^2(Q)}{(r + \bar{r})^2} \phi(\mathbf{r}), \quad (26)$$

where we reflect explicitly that when particles are separated by big distances  $r$ , the density of the multiparticle environment goes down in accordance with (25). The quantity  $c^2(Q)$  is defined in the following way

$$c^2(Q) = \frac{8\pi\alpha}{3} \frac{R_f^2 n_\pi}{T_f} \frac{v_{rel}^2}{v_{c.m.}^2}. \quad (27)$$

Fixing the screening radius at the freeze-out temperature and density as

$$R_{scr}^f = \sqrt{\frac{3T_f}{8\pi\alpha n_\pi}}, \quad (28)$$

we have

$$c(Q) = \frac{R_f}{R_{scr}^f} \frac{v_{rel}(Q)}{v_{c.m.}}. \quad (29)$$

In spherical coordinates, Eq.(26) can be rewritten as

$$\frac{d^2 \phi}{dr^2} + \frac{2}{r} \frac{d\phi}{dr} - \frac{c^2(Q)}{(r + \bar{r})^2} \phi(\mathbf{r}) = 0. \quad (30)$$

This equation has the following solution

$$\phi(r) = \frac{e}{r} \left( \frac{R_0}{r + \bar{r}} \right)^b, \quad (31)$$

where  $R_0$  is a scale parameter to fix the dimensions of the potential  $\phi$ . The exponent  $b$  is a solution of the quadratic equation resulting from the substitution of the ansatz (31) into Eq.(30) and takes the form (assuming a proper asymptotic behaviour of the potential  $\phi$ )

$$b = -\frac{1}{2} + \frac{1}{2} \sqrt{1 + 4c^2(Q)} \quad (32)$$

with  $b \rightarrow 0$  when  $n_\pi \rightarrow 0$  and, hence, the potential  $\phi(r)$  transforms to the Coulomb one in the absence of environment. The dependence of the exponent  $b$  on the relative momentum  $Q$  is shown in Fig. 3 when the LHC freeze-out conditions are taken. In the interval of interest, “ $b$ ” and, hence, deviations from a pure Coulomb field increase with the relative velocity. This intriguing behavior is directly related to the “Hubble-like” expansion implied by Eq. (24), and becomes quite understandable if we remember that the pion density decreases (hence  $R_{scr} \rightarrow \infty$ ) with  $R$  increasing. The expansion of the post freeze-out system thus results in modifications to the Coulomb potential that are of power-law, not exponential form, in contrast to that static result given by Eq. (8). We can treat the corrected potential obtained in Eq. (31) in terms of an effective charge distribution

$$e_{eff} = e \left( \frac{R_0}{r + \bar{r}} \right)^b, \quad (33)$$

We are going to average it by using the following procedure. If we confine our attention to  $v_{rel} \ll 1$ , Eq. (26) can be rewritten in a Poisson-like form  $(\nabla^2 - \kappa^2)\phi(\mathbf{r}) = 0$ , with  $\kappa \equiv c(Q)/(r + \bar{r})$ , which is equivalent to an  $r$ -dependent screening radius, i.e.,

$$R_{scr}(r) = \frac{r + \bar{r}}{c(Q)}. \quad (34)$$

Since, as shown in Fig. 3, the deviation of potential (31) from the pure Coulomb form in the region of small relative pion momenta  $Q \leq 30$  MeV is small, we first ignore the  $r$  dependence of  $\kappa$  to obtain the solution for the electromagnetic  $\pi\pi$  potential in the form of Eq. (8), then substitute the  $r$ -dependent  $\kappa$  into Eq. (8) to find

$$U_{\pi\pi} = \frac{\alpha e^{-c(Q)r/(r+\bar{r})}}{r}, \quad (35)$$

Thus, there is no exponential dependence of  $U_{\pi\pi}$  on  $r$  for large enough  $r$  (when  $r \gg \bar{r}$ ). Instead, the numerator on the r.h.s. of Eq. (35) represents the averaged charge

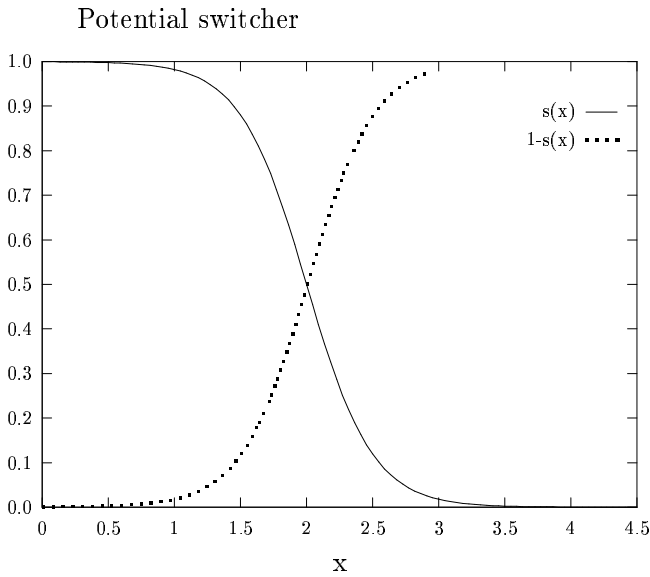


Fig. 4. Solid curve is the smooth potential switcher  $s(x) = \frac{1}{2} - \frac{1}{2}\tanh[2(x-2)]$ . Dotted curve is the alternative potential switcher  $1-s(x)$

distribution (33) squared (we are now considering the potential energy  $U_{\pi\pi}$  rather than the electric potential  $\phi$ ).

It is clear from Eq. (29) that when the ratio  $v_{\text{rel}}/v_{c.m} \ll 1$  ( $R_f$  and  $R_{\text{scr}}^f$  are of the same order for high multiplicities), the renormalized constant  $\alpha \exp[-c(Q)]$  is close to the bare value of  $\alpha$ . Moreover, the same qualitative result comes from the  $r$ -behavior of the screening radius (34) when it approaches the asymptotic value  $R_{\text{scr}} = \infty$  (Coulomb law) with increasing  $r$ . The quantity  $c(Q)$  increases with relative pion momentum leading to larger deviations from the Coulomb potential and agreement with the features of potential (31) (see discussion after Eq. (32)).

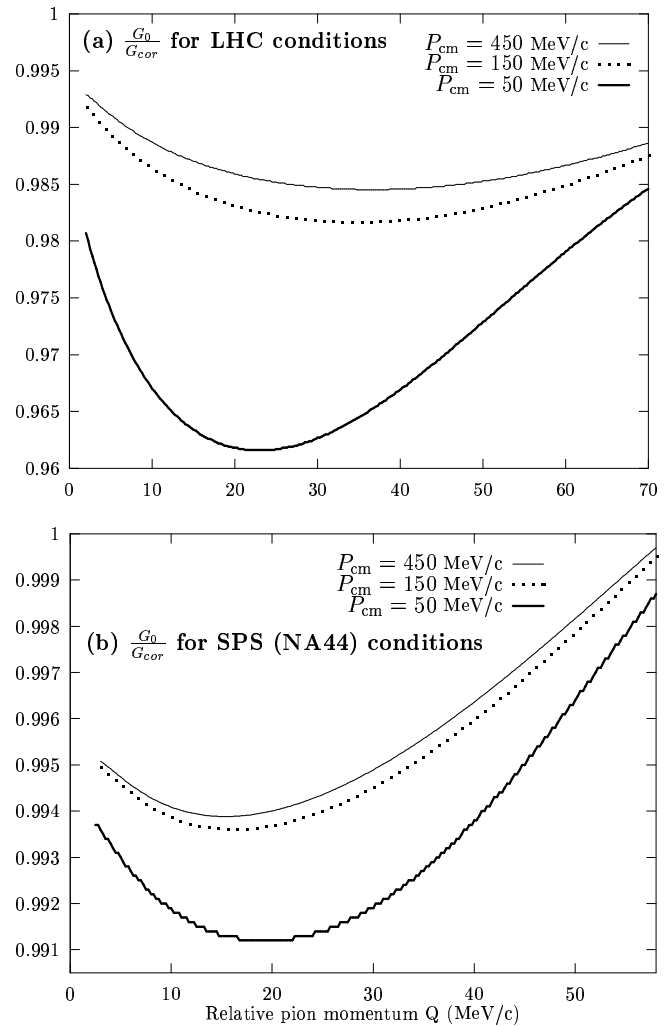
So, we deal with the two-particle potential

$$U_{\text{expan}}(r) = \frac{\alpha}{r} \left( \frac{R_0}{r + \bar{r}} \right)^b. \quad (36)$$

For evaluation, we take parameter  $R_0$  in the range  $R_0 = a_0 - 2a_0$ , where  $a_0$  is a mean distance between neighbor charged pions, which fixed at freeze-out.

But, before coming to numerical calculations, let us point out that the potential should be the Coulomb one at distances which are less than the mean distance between particles. Therefore, to improve a behavior of the potential in this range, we use a combination of two potentials by the smooth ‘‘potential switcher’’

$$s(x) = \frac{1}{2} - \frac{1}{2}\tanh[2(x-2)]. \quad (37)$$



Figs. 5. The ratio of the standard Gamov factor  $G_0$  and correction factor  $G_{\text{cor}}(Q) = |\psi(\mathbf{r} = 0)|^2$  which is obtained from solution of the Schrödinger equation with the use of potential (38). Curves depicted are evaluated for the different mean momenta of the pion pair in fireball frame:  $P_{c.m} = |\mathbf{p}_a + \mathbf{p}_b|/2$ . Fig. 5a: for LHC conditions -  $N_\pi = 8000$ ,  $T_f = 190$  MeV and  $R_f = 7$  fm; Fig. 5b: for SPS (NA44) conditions -  $N_\pi = 1000$ ,  $T_f = 190$  MeV and  $R_f = 7$  fm

which is depicted in Fig. 4. Then, incorporating the correct behavior of the potential at small distances, we obtain finally the potential energy in the following form

$$U_{\pi\pi}(r) = s(x) \frac{\alpha}{r} + [1-s(x)] U_{\text{expan}}(r), \quad (38)$$

where  $x = r/a_0$ . Certainly, with time evolution, the mean distance between particles will increase. But we

restrict our calculation to the freeze-out mean distance, which means that, in the competition between two potentials  $U_{\text{Coulomb}}$  and  $U_{\text{expand}}$ , we overestimate the contribution of the latter.

Results of the numerical solution of the Schrödinger equation with this potential energy give the correction factor  $G_{\text{cor}}(Q) = |\psi(\mathbf{r} = 0)|^2$ , which is depicted in Figs. 5a and 5b for the LHC and SPS freeze-out conditions correspondingly as a ratio with the standard Gamov factor  $G_0/G_{\text{cor}}$ . In fact, as it is seen, the deviation from the Gamov factor is small enough.

### 3. Summary and Conclusions

So, in our first approach, it was assumed the constant density of secondary particles which fill all space. In this case, our consideration shows that, for RHIC and LHC experiments, the screening radius of the Coulomb interaction at the freeze-out density and temperature could be comparable with the source size and therefore the factorization of Eq. (3) [2] is no longer valid. However, this conclusion changes drastically with the inclusion (switching on) of the expansion for the pion system which we mimic by appropriate density profile (12) of the post freeze-out medium. Actually, in our second model, we reduce the time evolution of two interacting pions to the stationary problem at the price of overestimation the density of the environment in which two probe particles move (see Fig. 2). Effectively, we consider the problem in the two-pion center-of-mass frame where the relative motion of particles which create the environment is slow enough in comparison to the radial collective expansion. It allows us to consider the stationary Schrödinger equation,  $(H_0 + V(r))\psi = E\psi$ , where  $V(r)$  is just electrical potential energy which we obtain solving Maxwell equation (7) for the scalar potential.

Kinematics of an expanding fireball reveals an important regulating parameter that is the ratio of the relative velocity of the detected pions and their center-of-mass velocity in the rest frame of a fireball,  $v_{\text{rel}}/v_{\text{c.m}}$  (see Eqs. (25) and (29)). We showed that the main contribution to the behavior of the correction factor in the region of small relative momentum comes from the behavior of the potential at large distances, which separate interacting particles. On the other hand, the two interacting particles are separated by a large distance when they far enough from the fireball where the density of the pion gas is small or even negligible. Hence, at this stage of evolution the two-particle potential is slightly (or even negligibly) distorted by

environment from the Coulomb one. As it seen from the Fig. 3, the magnitude of this distortion is partially regulated by the ratio  $v_{\text{rel}}/v_{\text{c.m}} \approx Q/P_{\text{c.m}}$ . The physical interpretation of this is transparent — as bigger the velocity of the pair  $v_{\text{c.m}}$  or its mean momentum  $P_{\text{c.m}}$ , as faster the pair leaves out the region of the dense environment leaving at the same time at small separated distance due to small relative velocity,  $v_{\text{rel}}$ . That is why, the long-range part of the two-pion potential, which is responsible for behavior of the correction factor at small relative momenta ( $Q \leq 50$  MeV), is practically not distorted and its behavior is very close to the long-range part of the Coulomb potential. Consequently, the correction factor for this region of the relative pion momentum should not practically deviate from the standard Gamov factor. Indeed, as it is seen from Figs. (5a) and (5b) the deviation of the evaluated correction factor from the Gamov factor is not more than several percent.

So, we showed that distortion of the Gamov factor, which is taken as an indicator of the final state Coulomb interaction, is practically negligible even if we overestimate the density of the secondary particles. We consider our result as an estimation of the influence of high secondary multiplicities on the two-particle final state Coulomb interaction. Account for these interactions is of great importance for interpretation of the interferometry experiments on SPS (CERN), RHIC (BNL) and future experiments on LHC (CERN). Work along further investigation of the effect of high multiplicities on the electromagnetic final state interactions is in progress.

One of the authors (D.A.) would like to acknowledge helpful discussions with U. Heinz. D.A. is indebted to the Secretariat and staff of CERN TH Division for support, warm hospitality and fruitful collaboration. This work was supported in part by the CERN TH Division Contract of Association and Regensburg University Project No.710008.

1. *Boal D.H., Gelbke C.-K., Jennings B.K.*//Rev. Mod. Phys. **62** (1990) 553.
2. *Gyulassy M., Kauffmann S.K., Wilson L.W.*//Phys. Rev. C. **20** (1979) 2267.
3. *Anchishkin D., Heinz U., Renk P.*//Ibid. **57** (1998) 1428.
4. *Barz H.W.*//Ibid. **53** (1996) 2536.
5. *Barz H.W., Bondorf J.P., Gaardhøje J.J., Heiselberg H.* [nucl-th/9711064].
6. *Sakharov A.D.*// Soviet JETP. **18** (1948) 631.
7. *Baier V.N., Fadin V.S.*//Ibid. **57** (1969) 225.



8. *Messiah A.* Quantum Mechanics. — Vol.1, North-Holland, Amsterdam, 1961.
9. *Akkelin S.V., Sinyukov Y.M.*//Phys. Lett. B. **356** (1995) 525.
10. *Chapman S., Scotto P., Heinz U.*//Heavy Ion Physics. **1** (1995) 1; *Wiedemann U.A., Scotto P., Heinz U.*//Phys. Rev. C. **53** (1996) 918.
11. *Anchishkin D., Zinovjev G.*//Phys. Rev. C. **51** (1995) R2306.
12. *Sinyukov Yu.M., Lörstadi B.*//Z. Phys. C. **61** (1994) 587.
13. *Satz H.*//Proc. LHC Workshop, vol. 1, CERN 90-10, Geneva, 1990.
14. *Atherton H., Boggild H., Boissevain J. et al.*//Nucl. Phys. A. **544** (1992) 125c.
15. *Anchishkin D.V., Zajc W.A., Zinovjev G.M.*//Ukr. J. Phys. **41** (1996) 363 [hep-ph/9512279].

Received 24.10.01

#### ВПЛИВ ВЕЛИКОЇ МНОЖИННОСТІ ВТОРИННИХ ЧАСТИНОК В РЕЛЯТИВІСТСЬКИХ ЗІТКНЕННЯХ ВАЖКИХ ІОНІВ НА ПИОН-ПИОННУ ВЗАЄМОДІЮ У КІНЦЕВОМУ СТАНІ

*Д.В. Анчишкін, В.А. Зайц, Г.М. Зинов'єв*

Резюме

Проведено дослідження впливу взаємодії у кінцевому стані на двочастинкові інклюзивні спектри, які спостерігаються під час ультрарелятивістських зіткнень важких ядер, в умовах великої множинності вторинних частинок (800—4000 вторинних пі-мезонів). Дослідження проблеми складається з декількох етапів. Перше, потрібно дослідити кінетику багаточастинкової системи після фріз-ауту (закінчення стадії еволюції, яка визначалася сильною взаємодією частинок системи). На основі аналізу розв'язків кінетичного рівняння пропонується квазістатична модель пост фріз-аут середовища, в якій контролювано завищується щільність частинок системи. В рамках цієї моделі вдається розв'язати рівняння Максвелла та знайти двочастинкову потенціальну енергію з урахуванням впливу середовища. Показано, що завдяки швидкому просторовому розширенню системи вторинних частинок, потенціал взаємодії двох пі-мезонів в такому плазмopodobному середовищі не екранований, як це важалось, а є показниковою функцією кулонівського типу. На другому етапі чисельно розв'язується двочастинкове рівняння Шредингера з використанням знайденого потенціалу. З допомогою хвильової функції, яка є розв'язком цього рівняння, визначається фактор Гамова. Ця величина є індикатором кулонівської взаємодії частинок у кінцевому стані. Отримано, що навіть для умов фріз-ауту, які характерні для експериментів на прискорювачах RHIC

та LHC, отриманий фактор Гамова відрізняється всього на декілька процентів від стандартного, визначеного для чисто кулонівської взаємодії. Зроблено передбачення, що висока вторинна множинність частинок практично не змінює характеру двочастинкової кулонівської взаємодії у кінцевому стані, а це, в цілому, має дуже важливе значення для інтерферометрії, де взаємодія у кінцевому стані суттєво впливає на двочастинкові спектри.

#### ВЛИЯНИЕ БОЛЬШОЙ МНОЖЕСТВЕННОСТИ ВТОРИЧНЫХ ЧАСТИЦ В РЕЛЯТИВИСТСКИХ СТОЛКНОВЕНИЯХ ТЯЖЕЛЫХ ИОНОВ НА ПИОН-ПИОННОЕ ВЗАИМОДЕЙСТВИЕ В КОНЕЧНОМ СОСТОЯНИИ

*Д.В. Анчишкин, В.А. Зайц, Г.М. Зиновьев*

Резюме

Проведено исследование влияния взаимодействия в конечном состоянии на двухчастичные инклюзивные спектры, которые регистрируются в ультрарелятивистских столкновениях тяжелых ядер, при высокой множественности вторичных частиц (800—4000 вторичных пи-мезонов). Исследование проблемы состоит из нескольких этапов. Первое, необходимо исследовать кинетику многочастичной системы после фриз-аута (конец стадии эволюции, которая определялась сильным взаимодействием частиц системы). На основе анализа решения кинетического уравнения предлагается квазистатическая модель пост фриз-аут среды, в которой контролировано завышается плотность частиц системы. В рамках этой модели удается решить уравнение Максвелла и найти двухчастичный потенциал, в котором учтено влияние среды. Показано, что благодаря быстрому пространственному расширению системы вторичных частиц, потенциал взаимодействия двух пи-мезонов в такой плазмopodobной среде не экранированный, как это считалось, а является показательной функцией кулоновского типа. На втором этапе численно решается уравнение Шредингера с использованием найденного двухчастичного потенциала. Волновая функция, которая является решением этого уравнения, определяет фактор Гамова. Последняя величина, в свою очередь, является индикатором кулоновского взаимодействия в конечном состоянии. Получено, что даже в условиях фриз-аута, которые характерны для экспериментов на ускорителях RHIC и LHC, получаемый фактор Гамова отличается всего на несколько процентов от стандартного, определяемого для чисто кулоновского взаимодействия. Сделано предсказание, что высокая множественность вторичных частиц практически не изменяет характера двухчастичного кулоновского взаимодействия в конечном состоянии, а это, в целом, имеет очень большое значение для интерферометрии, где взаимодействие в конечном состоянии существенным образом влияет на многочастичные спектры.